中國機械工程學刊第四十卷第四期第 341~353 頁(民國一百零八年)
Journal of the Chinese Society of Mechanical Engineers, Vol.40, No.4, pp 341~353 (2019)

Grinding Wheel Wear Monitoring Based on the Time Constant and Support Vector Machine

Yulun Chi*, Jiajian Gu**and Haolin Li*

Keywords: grinding wheel wear, the time constant, LS-SVM, wheel condition monitoring

Abstract

In cylindrical plunge grinding process, the wheel wear affects the form accuracy and surface quality of the workpiece. Therefore, monitoring the grinding wheel condition plays a key role in the quality of workpiece being manufactured. In this study, different typical sensors in grinding machines such as the dynamometer, acceleration, motor current and Acoustic Emission (AE) are in use for monitoring. The time constants of force, AE and power signals and the Mean Square Deviation (MSD) of accelerometer signals, are first acquired to study the grinding wheel wear process. Considering that it is not always easy to measure the wheel topography and the grinding surface roughness in real grinding process, the Least Square Support Vector Machine (LS-SVM) is introduced to monitor the grinding wheel wear in time to satisfy the grinding stringent requirements. A series of experiments was performed to verify that the monitoring method of wheel wear is effective and repeatable in grinding process control.

INTRODUCTION

Compared with other machining methods, high-performance plunge grinding process becomes one of the most complicated and important cutting processes as final machining stage. During a plunge grinding process, the grinding wheel rotating at a high speed moves only in a normal direction towards the workpiece that rotates at a much lower speed and such action results in a rapid reduction of workpiece size. Gao et al. [1] (1999) discussed that the grinding wheel performance condition affected the form accuracy and surface quality of the workpiece. It was suggested that the system monitoring and automation technology was much more necessary in order to supervise the process and detect the wheel conditions.

Due to the development of computer and sensing technology, many studies have been conducted to develop automated grinding wheel condition monitoring technologies to realize full automation of grinding operations. Couey et al. [2] (2005) incorporated non-contact displacement sensors into an aerostatic spindle that are calibrated to measure grinding forces from changes in the gap between the rotor and stator. The results indicate that the measurement method is capable of providing useful feedback in precision grinding with excellent contact sensitivity, resolution, and detection of events occurring. However, a direct measurement of the grinding force is limited due to the difficult installation of measuring instrument at the point of cylindrical plunge grinding. Liao et al. [3] (2007) presented a wavelet- based methodology for grinding wheel condition monitoring based on acoustic emission (AE) signals. The test results indicate that the proposed methodology can achieve 97% clustering accuracy for the high material removal rate condition, and 86.7% for the low material removal rate condition. Liao et al. [4] (2008) found that the best average classification accuracy of 91.9% was obtained using Adaptive Boosting-Minimum distance classifier. Liao et al. [5] (2010) used ant colony optimization-based method and the sequential forward floating selection method to choose the best feature subsets. It was found that the lowest classification error of 7.81% was achieved using center-based nearest neighbor for the dataset of wavelet energy feature, while the lowest classification error was 6.875% using the dataset of AR coefficients. Denkena et al. [6] (2014) found a new monitoring method for cylindrical plunge grinding wheel wear, which the recursive estimation can reduce noise. From above studies, typical sensors in grinding machines such as the displacement, acceleration, motor current

Paper Received February, 2017. Revised October. 2018. Accepted March, 2019. Author for Correspondence: Yulun Chi

* *Associate Professor,* ***Shanghai University for Science and Technology****, Shanghai200093,P.R. China.*

** *Gradnate Student,* ***Shanghai University for Science and Technology****, Shanghai200093,P.R. China.*

and acoustic emission are in use for monitoring. Nakai et al. [7] (2015) presented that acoustic emission and power signals were acquired during the tests, and the combination of signals and statistics along with the intelligent systems brings an innovative aspect to the grinding process. CHI et al. [8] (2016) found the relationship between the time constant and the grinding wheel performance. The increase of the time constant value with three consecutive grinding cycles could indicate that wheel surface deterioration occurs in the process represented by the wheel loading. These results indicate that the models are highly successful in estimating tool wear. A summary of grinding wheel condition monitoring is reported in Table.1.

Table.1 Summary of grinding wheel condition monitoring

Reference	Sensor(s)	Signal analysis	Features	Algorithm	Test results
Couey et al. [2] (2005)	Displacement	Force-based solution	Deflection	FFT	Below 1μm
Liao et al. [3] (2007)	AE	Wavelet analysis	Wavelet energy	Adaptive genetic clustering	97%(high MRR) 86.7%(low MRR)
Liao et al. [4] (2008)	AE	AR modeling	AR order	Boosted classifiers	91.9%
Liao et al. [5] (2010)	AE	AR modeling and Wavelet	AR order and wavelet energy	NM,KNN,FKNN, CBNN and KMNP	92.19%(wavelet features), 94.125%(AR coefficient)
Denkena et al.[6] (2014)	Displacement, acceleration, motor current and AE	Adaptive filter	Tool defects	The recursive estimation	Implement easily
Nakai et al. [7] (2015)	AE and power signals	Intelligent systems	Training and validating	Neural networks	highly successful
CHI et al. [8] (2016)	Power signal	Least-mean-squares	The time constant	Material removal rate	Not available

Our study differs from those above-reviewed studies in the following aspects: (1) A direct measurement of grinding force, AE, power and accelerometer signals were conducted to online monitor the cylindrical plunge grinding wheel conditions, which the grinding force was measured by the developed rotating dynamometer installed on the headstock of machine tool, the AE and accelerometer sensors on the tailstock center, and the power sensor installed in the electrical cabinet. (2) The time constant is an important parameter of grinding material removal system and is related with the grinding wheel conditions, so the force, AE and power signals are first analyzed by the time constant to study the grinding wheel wear process. And, the MSD of accelerometer signal is also used as parameter to evaluate the grinding wheel wear process. (3) To further study the analysis results of different monitoring signals, the grinding wheel topography and the workpiece surface roughness were directly measured to classify the wheel wear state by using the handled three-dimensional microscope and the laser-check scattered laser light sensor. (4) Due to the fact that it is not always easy to measure the wheel topography and the grinding surface roughness in real grinding process, the LS-SVM is introduced to monitor the grinding wheel wear in time to satisfy stringent requirements of surface roughness. The experimental results show the LS-SVM tool with input the parameters of signals is a feasible method with which to monitor grinding wheel wear condition. The overall structure of grinding wheel wear monitoring system is shown in Fig.1. In the following, a leading study was performed to monitor the grinding wheel conditions.

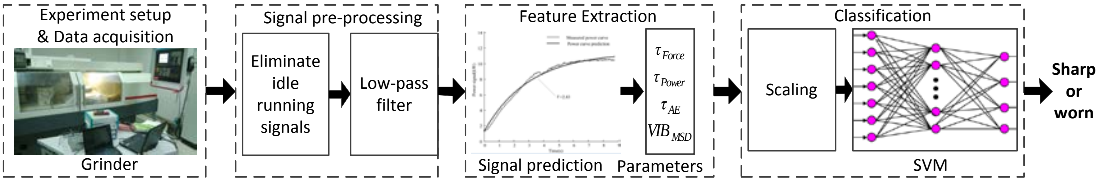

Fig.1 Structure of grinding wheel wear monitoring system

THE TIME CONSTANTESTIMATION

With the development of grinding monitoring system, sensors for process monitoring and control have been a technology which is used to provide efficient information on the grinding wheel conditions. Different sensors and parameters are described below.

The time constant

As confirmed by Chen et al. [10] (1996), the time constant of the plunge grinding system τ is a measure of the relationship between the system overall effective stiffness k_e and the grinding coefficient k_c. The time constant τ is expressed by:

$$\tau = \frac{k_c}{k_e n_w} \tag{1}$$

The above equation shows that the time constant τ is related to the overall effective stiffness k_e, the workpiece rotational speed n_w and the grinding force coefficient k_c. CHI et al. [8, 9] (2016) showed that the increase of the time constant value with consecutive grinding cycles could indicate that wheel surface deterioration. Therefore, it is possible to evaluate the wheel performance based on the time constant τ. In the following, different sensor signals are introduced to be used in monitoring grinding wheel wear process.

Sensors and parameters

In cylindrical plunge grinding process, the grinding forces of the tangential component, F_t, and a normal component, F_n can be acquired by using a developed tool dynamometer. The time constant τ can be calculated by following earlier work CHI et al. [9] (2016).

$$F_n = F_n' \approx \frac{k_c v_s \dot{u}_n}{n_w} \equiv K_S \qquad (t - t_{n-1} >> \tau) \tag{2}$$

$$\dot{F}_n = \frac{k_c v_s}{n_w \tau}(\dot{u}_n - \dot{u}_{n-1})e^{-1} \equiv \frac{K_S}{\tau}\left(1 - \frac{\dot{u}_{n-1}}{\dot{u}_n}\right)e^{-1}$$
$$(t-t_{n-1} = \tau, t-t_{n-2} >> \tau) \tag{3}$$

where, F_n is the steady-state force, $\dot{F}_n$ the rate of force change, v_s the grinding wheel speed, $\dot{u}$ the commanded infeed rate and n the order of the infeed stage. According to the Eqs. (2) and (3), the time constant τ can be expressed by:

$$\tau_{Force} = \frac{F_n}{\dot{F}_n}\left(1 - \frac{\dot{u}_{n-1}}{\dot{u}_n}\right)e^{-1}$$
$$(t-t_{n-1} = \tau, t-t_{n-2} >> \tau) \tag{4}$$

Lee et al. [11] (2003) reviewed that the grinding spindle power consumption provides an
indication of grinding torque and therefore, indirectly, of tool condition. The grinding power P associated with the normal grinding force F_n can be written as:

$$P = \frac{k_p F_n v_s}{k_{nt}} \tag{5}$$

where k_p is the coefficient of power, which depends on the grinding conditions, and k_{nt} the proportionality coefficient of the normal force and the tangential force. The time constant τ can be expressed by:

$$\tau_{Power} = \frac{P}{\dot{P}}(1 - \frac{\dot{u}_{n\text{-}1}}{\dot{u}_n})e^{-1} \qquad (t - t_{n\text{-}1} = \tau, t - t_{n\text{-}2} >> \tau) \quad (6)$$

An AE sensor sensitive to changes of the grinding state was selected for monitoring process. Tawakoli et al. [12] (2008) have found that a relationship exists between the AE RMS signal and the grinding process. Jiang et al. [13] (2014) supposed that the average AE RMS signal is proportional to the normal grinding force.

$$V_{AE} = k_{ae}F_n \quad (7)$$

where V_{AE} is the averaged AE RMS, and k_{ae} is the proportionality coefficient. The time constant τ can be expressed by:

$$\tau_{AE} = \frac{V_{AE}}{\dot{V}_{AE}}(1 - \frac{\dot{u}_{n\text{-}1}}{\dot{u}_n})e^{-1} \qquad (t - t_{n\text{-}1} = \tau, t - t_{n\text{-}2} >> \tau) \quad (8)$$

The aim of vibration monitoring is to found a deterioration process of the grinding wheel and a malfunction of the machine tool from the accelerometer signal. For this purpose, an acceleration sensor was adhered to machine tool tailstock center. The tailstock center amplitudes of acceleration signal by a *Mean* Square *Deviation*（MSD） were analyzed by Kang et al. [14] (2001).

$$VIB_{MSD} = \sqrt{\frac{\sum_{i=1}^{N}(x_i - \bar{x})^2}{N - 1}} \quad (9)$$

Where x_i is the extraction data, $\bar{x}$ the mean value and N the number of data satisfying the condition.

LEAST SQUARE SUPPORT VECTOR MACHINES

Using SVMs to judge the grinding wheel wear condition during grinding, would provide a rational test in developing a reliable tool for grinding process monitoring. An original SVM, may not be suitable in practice, due to its time consumption during the computation of quadratic programming. A least square SVM, was developed by Suykens and Vandewalle [15] (2002) for solving pattern recognition and non-linear function estimation problems. In this case, the LS-SVM is used to analyze different grinding monitoring signals and parameters. Once LS-SVM contains all needed information, the result can be predicted. The SVM equation modification developed by Suykens, is as follows:

Minimize: $$\frac{1}{2}\|\omega\|^2 + C\frac{1}{2}\sum_{i}^{l}\xi_i^2 \quad (10)$$

Subject to:

$$y_i((\omega \bullet x_i) + b) = 1 - \xi_i \text{，} \xi_i \geqslant 0, i = 1, \cdots, l. \quad (11)$$

Where ξ_i a non-negative slack variables. C is the coefficient, which is chosen by user. The weighting vector ω defines the direction of the separating hyperplane $f(x)$ as shown in Eq. (12).

$$f(x) = sign\{\omega \bullet x + b\} \quad (12)$$

Where the bias b defines the distance of the hyperplane from the origin.

The application of conditions for optimality yields the following linear KKT (Karush-Kuhn-Tucker) system:

$$\begin{bmatrix} 0 & y^T \\ y & \Omega + C^{-1}I \end{bmatrix}\begin{bmatrix} b \\ \alpha \end{bmatrix} = \begin{bmatrix} 0 \\ 1_v \end{bmatrix} \quad (13)$$

Where:

$$\Omega = Z^T Z, Z^T = (y_1\Phi(x_1), \cdots, y_n\Phi(x_n))$$

$$Y^T = (y_1, \cdots, y_n), 1_v = (1, \cdots, 1), \alpha = (\alpha_1, \cdots, \alpha_n)$$

Then:

$$\Omega = \psi(x_i, x_l) = \Phi(x_i)^T \Phi(x_l) i, l = 1, \cdots, N \quad (14)$$

By applying the kernel to the Ω matrix, classifier function estimation becomes:

$$f(x) = sign\{\sum_{i=1}^{l}\alpha_i y_i K(x_i, x_j) + b\} \quad (15)$$

Where $K(x_i, x_j)$ is the kernel function, which is shown as:

$$K(x_i, x_j) = \Phi(x_i)\Phi(x_j) \quad (16)$$

Where Φ is an actual mapping function. The study mainly focuses on the grinding wheel wear monitoring in this case. Then, the unknown data example is classified in the following way:

$$x\begin{cases} Class \quad I & if \quad f(x) = 1 \\ Class \quad II & if \quad f(x) = -1 \end{cases} \quad (17)$$

EXPERIMENTS

In this study, a series of experiments were performed using a computer numerically controlled (CNC) cylindrical grinding machine to study the grinding wheel wear process.

Machine tool conditions

Fig.2 shows a STUDER K-C33 multi-purpose CNC cylindrical grinding machine with an air-bearing workpiece spindle, and C45 steel with radius of 60mm was selected as the experimental material. The experiment was conducted to monitoring the wheel wear process by using four different sensor signals which are the force, the AE, the power and the accelerometer signals. The monitoring signals are filtered and digitised using a **DATAQ INSTRUMENTS DI-148U** data acquisition card. In the following sub-sections, different sensors setup is introduced in the grinding monitoring system. The parameters of the grinding wheel and workpiece are shown in Table.2.

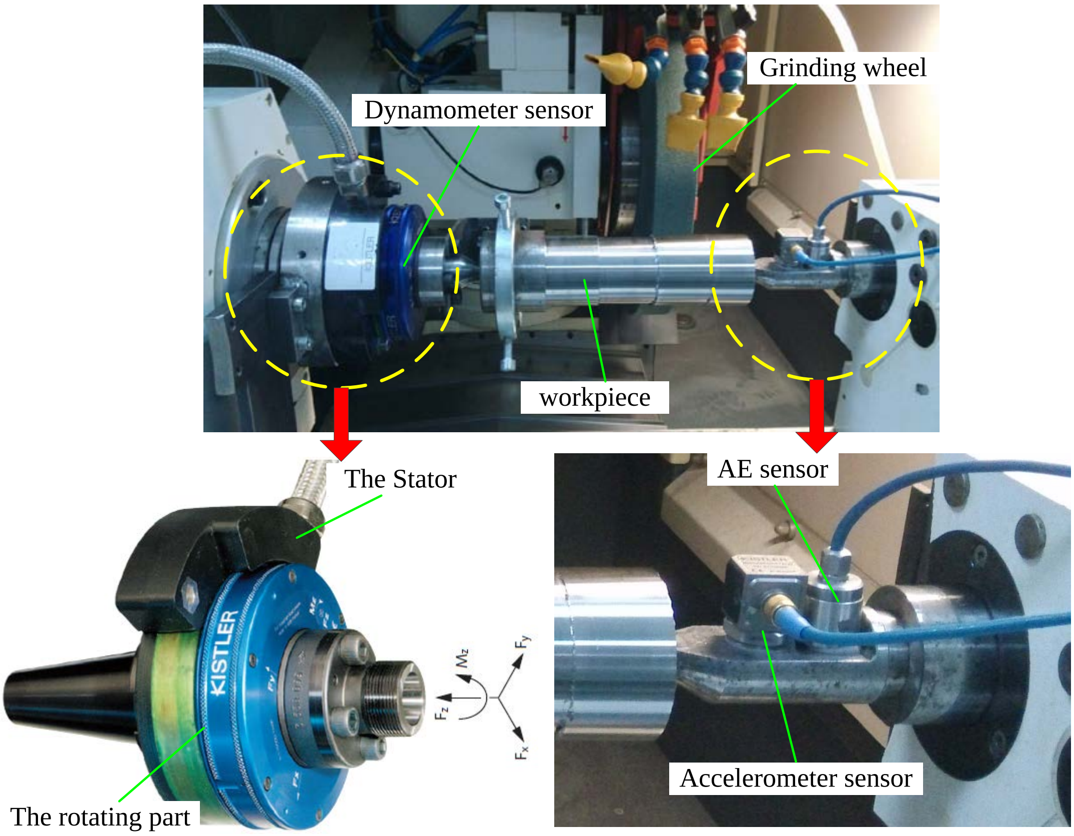

Fig.2 Experiment setup and the monitoring sensors

Table.2 the parameters of the grinding wheel and workpiece

Parameter	Property
Worpiece material	C45
Wheel material	Vitrified aluminum oxide
Workpiece dimension(mm)	Φ75.2(diameter)×200(length)
Wheel dimension(mm)	Φ600(diameter)×56(width)×Φ220(bore)
Worpiece speed(r/min)	120
Wheel speed(m/s)	33

Sensors and measurement

The detailed specification of the dynamometer instrument is given in Fig.2. A dynamometer sensor KISTLER 9123C which consists of a four component sensor fitted under high preload between a baseplate and top plate , is especially suitable for installing on the spindle stock to measure the grinding force. The type 8395A triaxial capacitive accelerometer is installed on the machine tool tailstock and utilizes a silicon Micro-Electro-Mechanical System (MEMS) variable capacitance sensing element to test the grinding workpiece vibration. The type SBS AE-1000 which consists of a custom designed electronic control system is used to detect high frequency acoustic emissions generated in the machine structure resulting from the grinding or grinding process. The electric spindle power was measured using a power sensor LOAD CONTROL PH-3A installed in a machine tool electrical cabinet as shown in Fig.3.

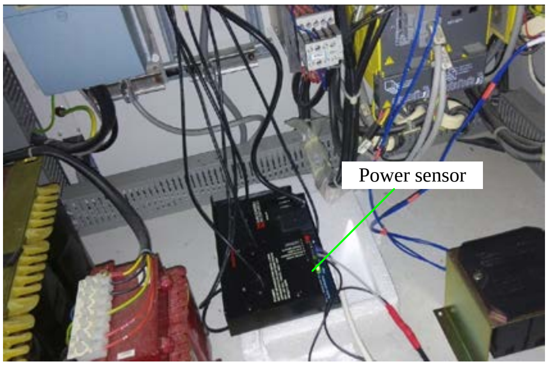

Fig.3 The power sensor setup

The grinding wheel surface microtopography is conveniently tested by using handled three-dimensional microscope as shown in Fig.4. The KENYCE VHX 3000 is an all-in-one microscope that incorporates observation, image capture, and measurement capabilities. As shown in Fig.5, the laser-check scattered laser light sensor is easy used to test the workpiece surface roughness by hand after grinding. In high volume surface finishing operations such as grinding, laser-check 6212B can quickly and easily check product surfaces, ensuring process and quality control. As shown in Fig.5, the laser-check scattered laser light sensor is easy used to test the workpiece surface roughness by hand after grinding. In high volume surface finishing operations such as grinding, laser-check 6212B can quickly and easily check product surfaces, ensuring process and quality control.

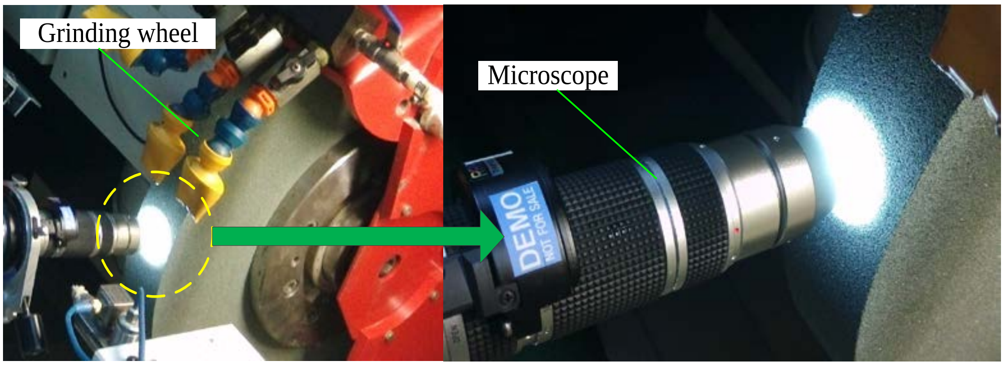

Fig.4 Grinding wheel surface test

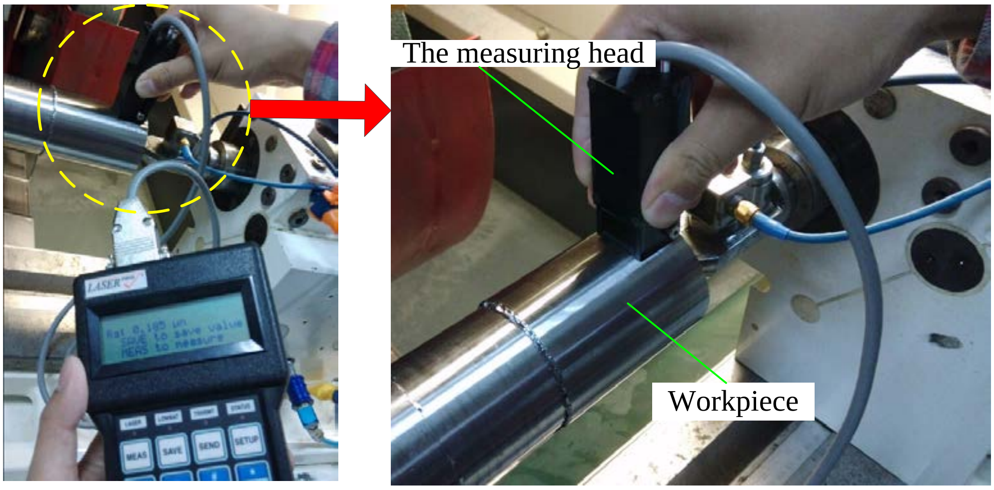

Fig.5 Grinding surface roughness measurement

To test the validity of the experimental results, a lot of consecutive grinding cycles, with infeed rate of 12μm/s and 8μm/s after the wheel dressing, were performed to study the wheel topography and the grinding workpiece surface roughness in terms of grinding wheel wear. In each whole grinding cycle, the spark-out stage lasted 10s as shown in table.3, and four different sensor signals which are the force, the AE, the power and the accelerometer signals were measured by using the method of Fig.2 and Fig.3. At the end of each grinding cycle, the grinding wheel topography and the workpiece surface roughness were recorded by using the equipment of Fig.4 and Fig.5. After consecutive grinding cycles, the monitoring signals were analysed for the grinding wheel wear process.

Table.3 The experiment grinding parameters

Infeed allowance（mm）	Infeed speed（μm/s）	Spark-out time（s）
0.1	12	10
0.1	8	10

EXPERIMENT RESULTS AND DISCUSSION

This discussion is divided into three parts based on the experimental work. First, the experimental procedure is introduced to acquire the measurement data in terms of grinding wheel wear process. The monitoring signals of different sensors were collected to study the relationship between the signal parameters and the grinding wheel wear process during the consecutive grinding cycles. From the signal analysis results, it found that these parameters contain the grinding wheel wear information. Second, to classify the grinding wheel sharp or worn more accurately, the grinding wheel topography and the workpiece surface roughness were measured to further analyse the results of the section 5.1. At last, the LS-SVM is introduced to monitor the grinding wheel wear in time to satisfy the grinding stringent requirements. The input parameters of the SVM were the time constants of force, power and AE signals, and the MSD of accelerometer signals. The classification results indicate that the LS-SVM tool with input parameters of signals is a feasible method with which to monitor grinding wheel wear condition.

Results of signal analysis in wheel wear process

After redressing, the grinding wheel is sharp during the first grinding cycle as shown in Fig.6. It can be seen that the infeed stage of signals (force, AE and power) can be divided into the rising stage and the steady state. This is because that the elastic deflection between the wheel and workpiece are generated at the beginning of the infeed grinding, and the grinding force is rising at this stage. When the infeed grinding reaches a steady state, the deflection and the grinding force do not change. Due to different sensor characteristic, the rising stage time t_s is also different for force, AE and power signals, which are 3.8s, 2.2s and 4.7s. During the first grinding cycle, the vibration signal is not obvious, and the maximum of accelerometer signal $VIB_{\max}$ is about 0.548m/s^2.

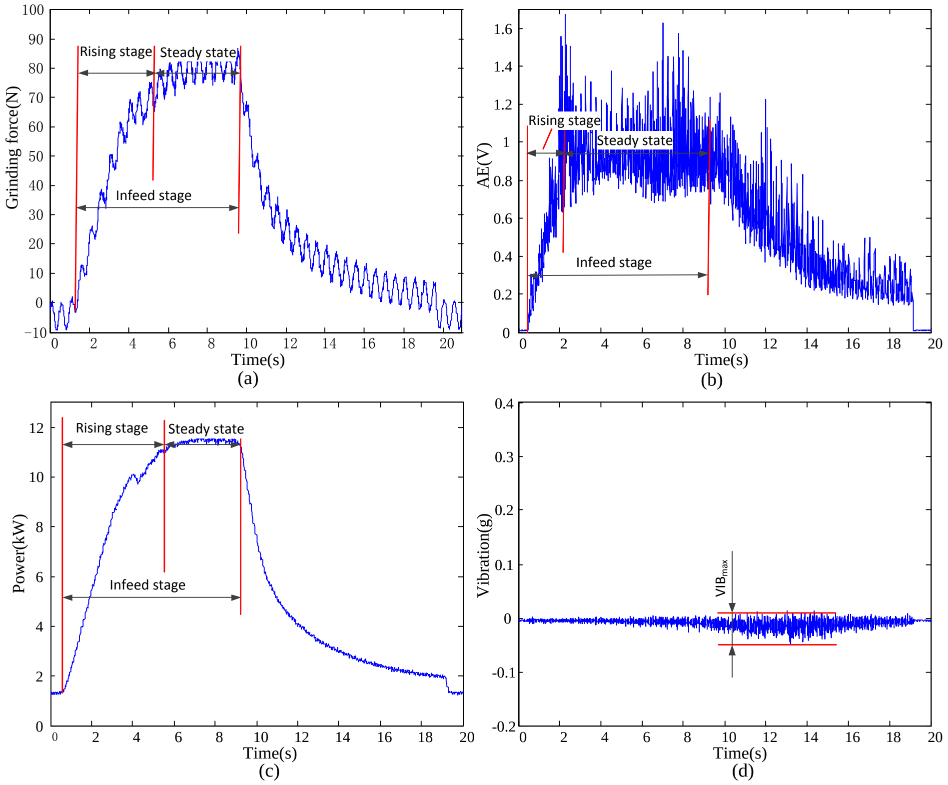

Fig.6 The monitoring signals during the first grinding cycle: (a) force, (b) AE, (c) power, (d) accelerometer

To reduce the effect of measuring noise, the least-mean-squares (LMS) estimation method is applied to power signal sample as shown in Fig.7. A portion of the infeed LMS power data was selected to calculate the time constant of power signal by using Eq. (4), and thus, the predicted power curve can be acquired with the previous studied model [9]. Through the comparison between the predicted and the measured power curves, it demonstrates that the time constant τ can be estimated exactly. For the twenty-one grinding cycles, the time constants of force, AE and power infeed stage signals can be separately estimated [10, 13] with the similar methodby using above Eqs. (4), (6) and (8). And, the MSD of vibration signals is calculated by Eq. (9). These parameter changing curves for monitoring grinding wheel condition during twenty-one grinding cycles in both the sharp and the wear conditions were shown in Fig.8.

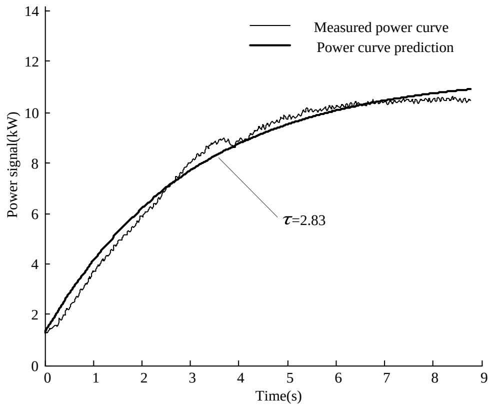

Fig.7 Comparison between the predicted and measured power curves

With consecutive grinding cycles, the grinding wheel surface wears out more and more seriously. From the Fig.8 (a), (b) and (c), the different time constant changing curve trends were similar, and all of them have obvious increasing after about 9-12 grinding cycles. From these results, it can be inferred that the cutting ability of the grinding wheel becomes weak, and the wheel abrasive wears more and more seriously. And, the MSD of accelerometer signal was also compared and illustrated in Fig.8 (d). Similar with the time constant results, there is also an obvious increasing after about 9-12 grinding cycles. From the signal analysis, the parameters of monitoring signals are increasing with the grinding time but are not proportional to the grinding cycles. In fact, the results show the parameters of monitoring signals increases with somewhat a change in the whole grinding process as show the green cycle in Fig.8. And, these parameters are impossible to predict the wheel wear accurately. Therefore, it is difficult to evaluate the wheel performance directly by setting the threshold line for different parameters to control dressing automatically to assure the grinding quality well.

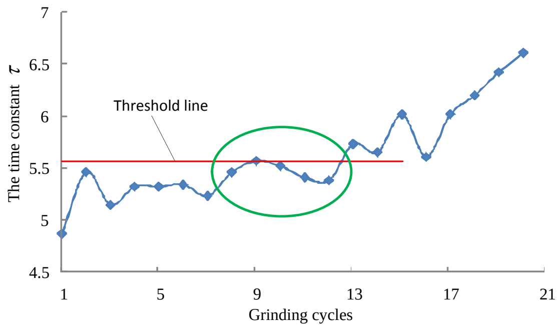

(a)

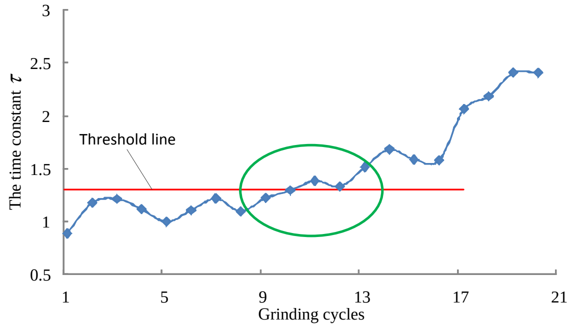

(b)

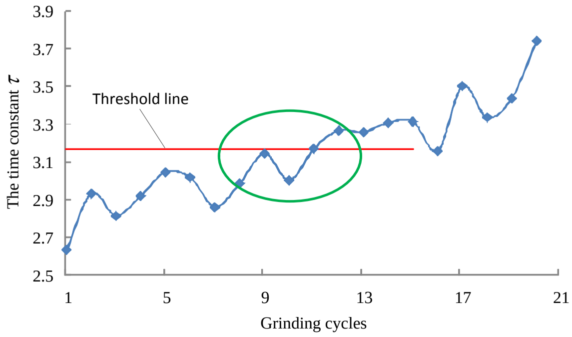

(c)

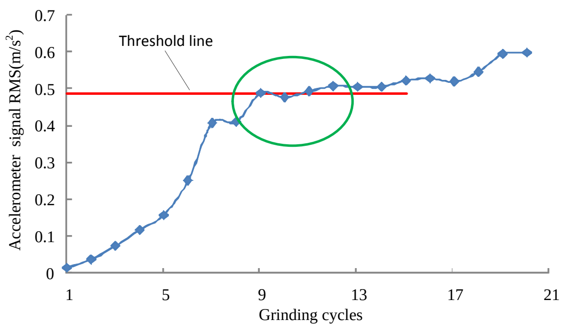

(d)

Fig.8 The parameters changing according to the wheel wear process: (a) the time constant of force signal, (b) the time constant of AE signal, (c) the time constant of power signal, (d) the MSD of accelerometer signal

As shown in Fig.9, the monitoring signals of different sensors are presented during the last or 21th grinding cycles. Due to the wheel wear seriously, these signals are different with the first grinding cycle's. Compared with Fig.6, it can be seen that the infeed stage only includes the rising stage for the force, AE and power signals as shown in Fig.9 (a), (b) and (c). This is because that the grinding wheel wears out seriously, the infeed grinding cannot reach a steady state. In the whole infeed stage, the grinding force does not reach the balance, and the grinding quality will be affected. Compared with Fig.6 (d), there is an intense vibration of machine stock for the Fig.9 (d), and the maximum of accelerometer signal VIB_{max} is about 6.02m/s^2 more than ten times of the Fig.6 (d)'s result.

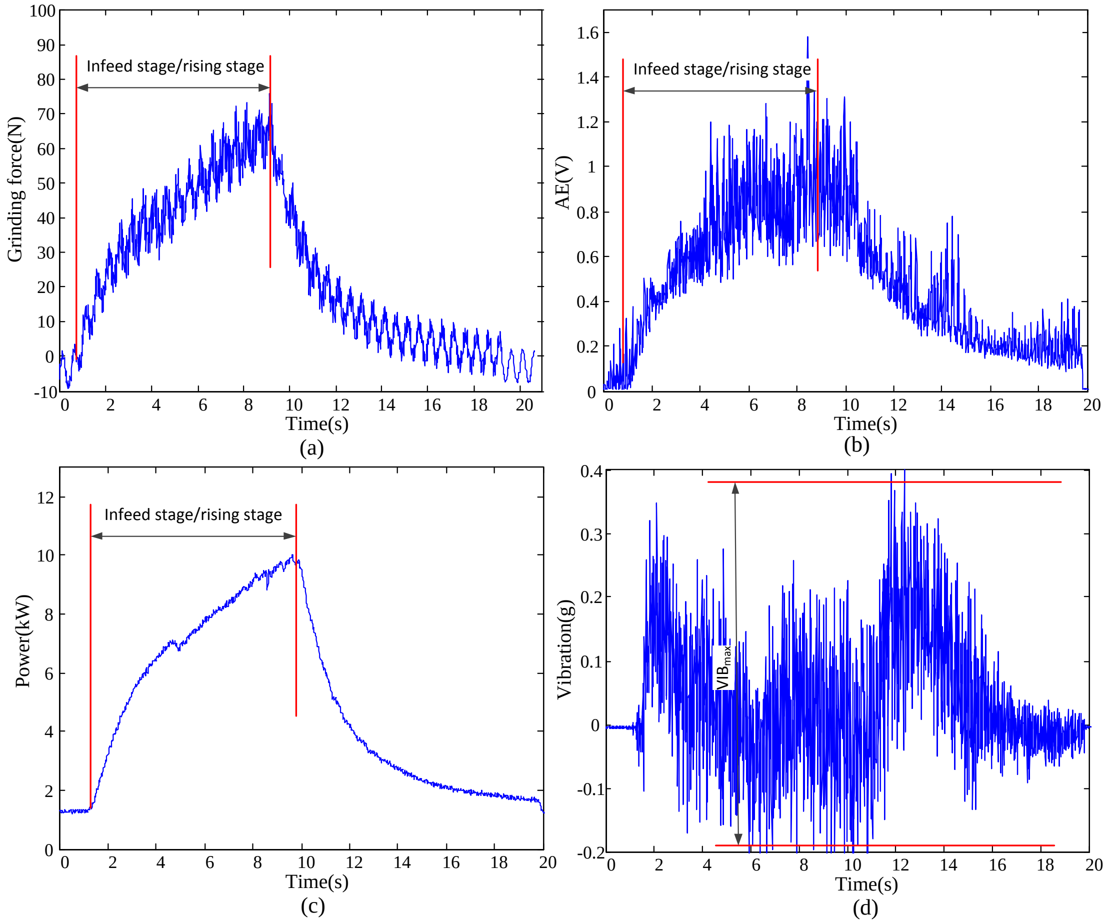

Fig.9 The monitoring signals during the last grinding cycle: (a) force signal, (b) AE signal, (c) power signal, (d) accelerometer signal

From the result of signal analysis in the grinding wheel wear, it can be inferred that the different parameters of monitoring signals have similar trend with the grinding wheel wear process. These parameters contain the grinding wheel wear information. Due to the processing uncertainty, one of these parameters is very difficult to represent for the grinding wheel condition change. SVMs have been recognized as powerful machine learning tools, with good theoretical properties for convergence and generalization. Thus, the different parameters of monitoring signals are selected as input of SVM to predict the grinding wheel wear process more accurately. To classify the grinding wheel sharp or worn more accurately, the measurement results of grinding wheel topography and surface roughness would be studied in the following section.

The wheel topography and the roughness analysis

As shown in Fig.10 and Fig.11, the wheel surface topography and the grinding surface roughness during the twenty-one grinding cycles, were acquired to further analyse the results of the section 5.1. The situation with the wheel surface topography is changing for different grinding cycles. After new redressing, the grinding wheel surface is clear to keep cutting ability well as shown in Fig.10 (a). With consecutive grinding cycles, the stuck chips in the grinding wheel surface are increasing as shown in Fig.10 (b) and (c). After 12 grinding cycles, the stuck chips in the grinding wheel surface are very seriously and affecting the wheel performance as shown in Fig.10 (d). With more grinding cycles, the grinding wheel surface wears out completely as shown in

Fig.10 (e) and (f), and needs more grinding force to remove material. As can be seen in the Fig.10, the results are almost consistent with the analysis results of Fig.8.

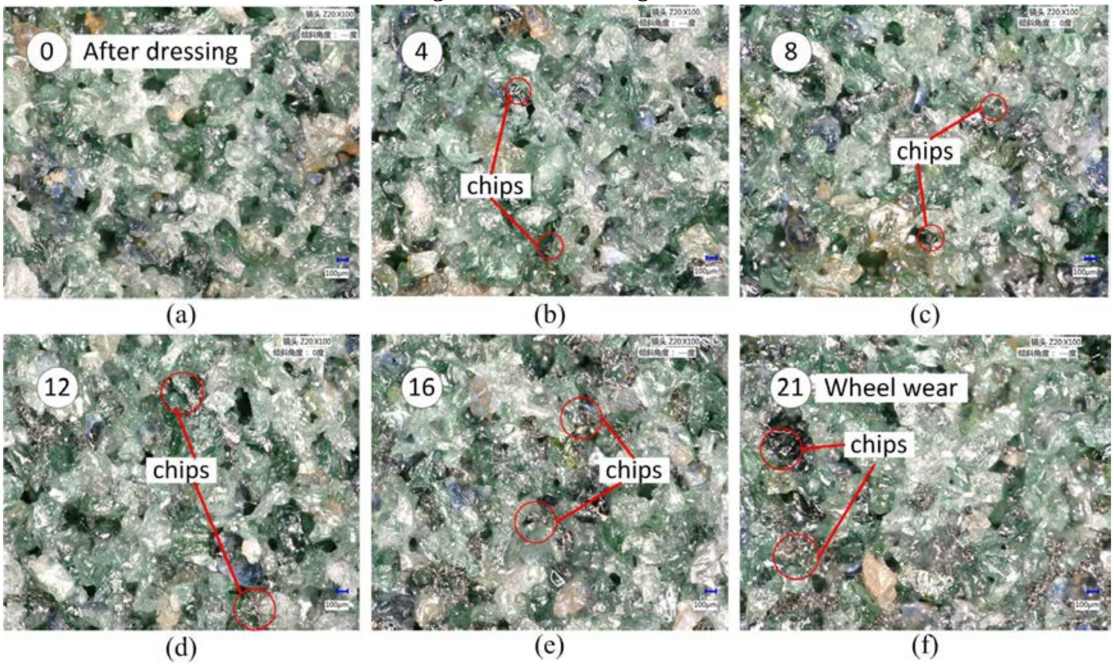

Fig.10 The wheel surface change with grinding cycles: (a) the wheel surface after dressing, (b) the wheel surface after the 4th cycle, (c) after the 8th cycle, (d) after the 12th cycle, (e) after the 16th cycle, (f) after the 21th cycle

The grinding workpiece roughness is also changing with the performance of the grinding wheel. Because, the surface roughness result is different at each measurement position, the fitting surface roughness is calculated by the least square method in this experiment. The target surface roughness is that the fitting surface roughness reach the maximum. This part is mainly concerned with the fitting surface roughness curve during the 21 grinding cycles as shown in Fig.11. At the beginning, the fitting surface roughness is increasing with consecutive grinding cycles. When the grinding cycles is more than twelve times, it can be seen that the fitting results reach the maximum line and don't change obviously, which can be observed clearly by the fitting curve. The explanation of this phenomenon is that the grinding wheel wears out completely after twelve grinding cycles. And, the fitting grinding surface roughness is not increasing with more grinding cycles.

From the wheel topography and the grinding surface roughness analysis, the results of signals analysis in the section 5.1 are further verified. It further proved that different sensor signals in cylindrical plunge grinding are efficient in the condition monitoring of the grinding wheel wear. In the experiment, the wheel state is classified into two categories: sharp and worn, was observed in the 12 grinding cycles. After 12 grinding cycles, the wheel is worn.

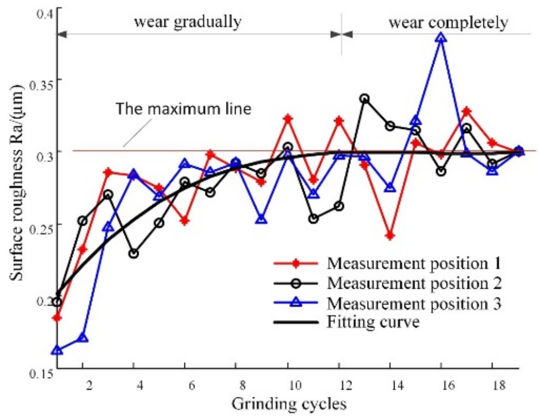

Fig.11 The grinding workpiece surface roughness results

For many practical applications, the reliability of the cycles is often critically dependent upon the surface quality by grinding. Due to the fact that it is not always easy to measure the wheel topography and the grinding surface roughness in real grinding process, the LS-SVM is introduced to monitor the grinding wheel wear in time to satisfy stringent requirements of surface roughness.

The LS-SVM classification results

The LS-SVM was used to predict grinding wheel wear, and analysis was carried out using a MATLAB

LS-SVM toolbox. The states of grinding wheel are classified into two categories: sharp and worn, which were designed as the output of our pattern recognition system. A Radial Basic Function (RBF) kernel was selected for classification, where the LS-SVM gives 1 for wheel sharp and -1 for wheel worn. The input parameters of the SVM were the time constants of force, power and AE signals, and the MSD of accelerometer signals. Therefore, feature vector is constructed by $\lfloor \tau_{Force}, \tau_{Power}, \tau_{AE}, VIB_{MSD} \rfloor$ under two infeed rates and set as inputs for the SVM classification. Table.4 and table.5 show 10 sets of data about the input parameters of monitoring signals and the output wheel states with infeed rate of 8μm/s and 12μm/s.

In this study, two groups of feature vectors extracted from different signals using above methods were input in the SVM classification system. According to the practical cylindrical plunge grinding process, the wheel wear is always supervised under the same grinding condition. So, the separated classifier is used for each infeed rate. In this experiments, the 104 grinding cycles with infeed rate of 8μm/s and 12μm/s were carried out to collect the signals for testing the performance of the proposed methodology. The first feature vector had 30 records of sharp conditions and 32 records of worn conditions with the infeed rate of 8μm/s, while the other set had 18 records of sharp conditions and 24 records of worn conditions with the infeed rate of 12μm/s. Half records of each feature vector were taken out for training and the other half for testing.

Table.4 Parameters of monitoring signals, the infeed rate=8μm/s

No.	**states**	τ_{Force}	τ_{Power}	τ_{AE}	VIB_{MSD}
1	Sharp (1)	2.2744	0.80377	0.028167	4.2713
2	Sharp (1)	2.5286	0.96756	0.091799	4.7934
3	Sharp (1)	2.1952	0.96386	0.24359	4.1317
4	Sharp (1)	2.4419	1.0418	0.41406	4.0371
5	Sharp (1)	2.6407	1.1653	0.46055	5.077
6	Worn (-1)	2.322	1.1638	0.48951	5.146
7	Worn (-1)	2.4268	1.5063	0.50393	5.0614
8	Worn (-1)	2.5999	1.4858	0.53687	4.9745
9	Worn (-1)	2.7099	2.1125	0.55076	5.3696
10	Worn (-1)	3.1623	2.1546	0.59974	5.6193

Table.5 Parameters of monitoring signals, the infeed rate=12μm/s

No.	**states**	τ_{Force}	τ_{Power}	τ_{AE}	VIB_{MSD}
1	Sharp (1)	2.6142	0.8963	0.0147	4.8532
2	Sharp (1)	2.7999	1.2318	0.0754	5.1372
3	Sharp (1)	3.0353	1.0095	0.1608	5.3174
4	Sharp (1)	2.8452	1.2341	0.4167	5.2271
5	Worn (-1)	3.1369	1.2399	0.5	5.5691
6	Worn (-1)	3.163	1.4072	0.5048	5.4064
7	Worn (-1)	3.2528	1.5383	0.5172	5.7373
8	Worn (-1)	3.3103	1.6115	0.5349	6.0275
9	Worn (-1)	3.5031	2.1005	0.5316	6.0295
10	Worn (-1)	3.4375	2.4542	0.6085	6.4433

Table.6 shows the classification results under the two grinding conditions. The classification accuracy was 96.67% under the infeed rate of 8μm/s. With the infeed rate of 12μm/s, the accuracy is much higher, which was 100%. The classification results indicate that the LS-SVM tool with input feature vectors of signals is a feasible method with which to monitor grinding wheel wear condition.

Table.6 Classification results

Infeed rate is 8μm/s				Infeed rate is 12μm/s			
States	Prediction amount	Target amount	Result	States	Prediction amount	Target amount	Result
Sharp	15	16	96.67%	Sharp	9	9	100%
Worn	16	14		Worn	12	12	

CONCLUSIONS

For cylindrical plunge grinding process, different sensor signals and LS-SVM have been presented to monitor the grinding wheel wear process in this paper. The presented methodology involves collecting force, AE, power and accelerometer signals in grinding at different wheel states, taking the time constants from force, AE, and power signals, extracting the MSD from the accelerometer signals. To classify the grinding wheel sharp or worn more accurately, the grinding wheel topography and the workpiece surface roughness were also measured to put each signal feature into one of two wheel states: 'sharp' and 'worn'. The LS-SVM was used to predict grinding wheel wear, and analysis was carried out using a MATLAB LS-SVM toolbox.

Grinding experiments were carried out to collect the signals for testing the performance of the proposed methodology. The test results show the classification accuracy was 96.67% under the infeed rate of 8μm/s. With the infeed rate of 12μm/s, the accuracy is much higher, which was 100%. It was confirmed that the LS-SVM tool with input feature vectors of signals can identify the wheel condition with high accuracy under different grinding conditions. For many practical applications, this study can be used to evaluate the wheel performance for different signal parameters to control dressing automatically to assure the grinding quality. Furthermore, more experiments will be necessary to optimise the grinding parameters in terms of the total grinding time or total grinding cost. The grinding optimisation process will be studied in detail in future work.

Funding

This work was financially supported by the National Science and Technology Support Program (2013ZX04008-011).

References

Gao, Y., Jones,B. "Fast time constant estimation for plunge grinding process control," *Int. J. Mach. Tools Manuf*,1999,39 (1): 143-156.

Couey, J.A., Marsh, E.R., Knapp, B.R., Vallance, R.R.. "Monitoring force in precision cylindrical grinding," *Precis. Eng*.,2005,29 (3): 307-314.

Liao, T.W., Ting, C.F., Qu, J., Blau, P.J. "A wavelet-based methodology for grinding wheel condition monitoring," *Int. J. Mach. Tools. Manuf*,2007 47 (3-4): 580-592.

Liao, T.W., Tang, F., Qu, J., Blau, P.J. "Grinding wheel condition monitoring with boosted minimum distance classifiers," *Mech. Syst. Signal*,2008,Pr. 22 (1): 217 – 232.

Liao, T.W."Feature extraction and selection from acoustic emission signals with an application in grinding wheel condition monitoring," *Eng. Appl. Artif. Intell*,2010, 23:74–84.

Denkena, B., Ortmaier, T., Ahrens, M., Fischer, R., "Monitoring of grinding wheel defects using recursive estimation," Int. J. Adv. Manuf. Technol.,2014,75 (5-8): 1005-1015.

Nakai, M.E., Aguiar, P.R., Guillardi, H., Bianchi, E.C., Spatti, D.H.,. "Evaluation of neural models applied to the estimation of tool wear in the grinding of advanced ceramics." *Expert. Syst Appl*.2015, 42 (20): 7026-7035.

CHI, Y., LI, H., Chen, X. "In-Process Monitoring and Analysis of Bearing Outer Race Way Grinding based on the Power Signal," *Proc. IMechE Part B: J Engineering Manufacture*,2016,3 (1): 1–14.

CHI, Y., LI, H. "A general material removal model for multi-infeed internal plunge grinding by using power signal," *J. Chin. Soc. Mechn. Eng*, 2016,Vol. 37, No.4: 359–365.

Chen, X., Rowe, W.B., Mills, B., Allanson, D.R. "Analysis and simulation of the grinding process. Part III. Comparison with experiment." *Int. J. Mach. Tools. Manuf*,1996,36 (8): 897–906.

Lee, E.S., Kim, J.D., Kim, N.H. "Plunge grinding characteristics using the current signal of spindle motor," *J. Mater. Process. Technol*,2003, 132 (1-2): 58-66.

Tawakoli, T. "Developments in grinding process monitoring and evaluation of results," *Int. J. Mech. Manuf .Syst*,2008, 1(4): 307 – 320.

Jiang, C., Li, H., Mai. Y., Guo, D. "Material removal monitoring in precision cylindrical plunge grinding using acoustic emission signal," *Proc. IMechE. Part C: Journal of Mechanical Engineering Science*,2014, 228 (4): 715-722.

Kang, M.C., Kim, J.S., Kim, J.H. "A monitoring technique using a multi-sensor in high speed machining," *J. Mater. Process. Technol*,2001, 113 (1-3): 331-336.

K. Pelckman, J. A. K. Suykens, T. V. Gestel, J. D Brabanter,L. Lukas, B. Hamers, B. D. Moor, J. Vandewalle. "A Matlab/c toolbox for least square support vector machines," *ESAT-SCD-SISTA Technical Report*, 2002,02-145.

NOMENCLATURE

τ time constant of the plunge grinding system

k_e system overall effective stiffness

k_c grinding coefficient

n_w workpiece rotational speed

F_t grinding forces of the tangential component

F_n steady-state force

$\dot{F}_n$ rate of force change

v_s grinding wheel speed

$\dot{u}$ commanded infeed rate

n order of the infeed stage

P grinding power

k_p coefficient of power

k_{nt} proportionality coefficient of the normal force and the tangential force

V_{AE} averaged AE RMS

k_{ae} proportionality coefficient

x_i the extraction data

$\bar{x}$ mean value

N number of data satisfying the condition

ξ_i non-negative slack variables

C coefficient, which is chosen by user

ω The weighting vector

b distance of the hyperplane from the origin

$K(x_i, x_j)$ kernel function

Φ an actual mapping function

基於時間常數和支援向量機的砂輪磨損監測

遲玉倫　顧佳健 李郝林
上海理工大學機械工程學院

摘 要

在外圓切入式磨削過程中，砂輪磨損會影響工件的形狀精度和表面品質，線上監測砂輪磨損狀態對於保證工件品質起著關鍵作用。本研究基於不同的感測器信號，如，力、功率、加速度、電機電流和聲發射（AE）等對數控磨床來進行線上監測。通過計算磨削力、AE 和功率信號的時間常數以及加速度信號的均方偏差（MSD）來研究砂輪磨損過程。由於實際磨削過程中測量砂輪形貌和磨削表面粗糙度反應砂輪磨損過程較為複雜且難以實施，本文則採用最小二乘支持向量機（LS-SVM）結合採集信號參數來即時監控砂輪磨損，以滿足磨削加工各項指標要求。最後，通過大量實驗驗證了該砂輪磨損監測方法在磨削程序控制中的有效性和可靠性。